

Research Article

Estimation of Climatic Parameters of a PV System Based on Gradient Method

Rabiaa Gammoudi ¹, Houda Brahmi ² and Rachid Dhifaoui³

¹Department of Electrical Engineering, National High School of Engineering of Tunis (ENSIT), Avenue Taha Hussein Montfleury, 1008 Tunis, Unit of Research ERCO-INSAT, Tunisia

²University Tunis el Manar, Higher Institute of Medicals Technologies of Tunis (ISTMT), 9 Rue Zouhair Essafi, 1006 Tunis, Unit of Research ERCO-INSAT, Tunisia

³University of Carthage, National Institute of Applied Sciences and Technologies, Centre Urbain Nord BP 676, 1080 Tunis Cedex, Unit of Research ERCO-INSAT, Tunisia

Correspondence should be addressed to Houda Brahmi; houda.brahmi@istmt.utm.tn

Received 25 October 2018; Revised 2 January 2019; Accepted 28 January 2019; Published 18 February 2019

Guest Editor: Aitor J. Garrido

Copyright © 2019 Rabiaa Gammoudi et al. This is an open access article distributed under the Creative Commons Attribution License, which permits unrestricted use, distribution, and reproduction in any medium, provided the original work is properly cited.

The behavior of a photovoltaic generator is generally described by its current-voltage characteristic whose appearance depends on the climatic conditions (temperature and solar radiation). The aim of this work is to show the possibility of identifying the values of these two parameters from an experimental curve $I_{pv}(V_{pv})$ using numerical method. Subsequently, we will also estimate the series and shunt resistors of the equivalent scheme of a PVG. This estimate is certainly beneficial to properly evaluate its energy balance. The integration of these resistances allows us to obtain a new model. In this work, we will propose a mathematical calculation strategy to ensure the estimation of all the parameters.

1. Introduction

It is now recognized internationally that the supply of energy, in its various forms, contributes to the sustainable development of the countries. In this context, fossil fuels (oil, gas, uranium, etc.), despite their contributions, have disadvantages in terms of capacity that comes from the deterioration of the world's reserves and in terms of the impact on the environment. The latter is visible by the rejection of greenhouse gases that causes global warming. These disadvantages give rise to technologies that help the exploitation of inexhaustible clean natural energies. In recent decades, as a result of improved panel performance, photovoltaic, as well as the progression of benefits including subsidies, the profitability of a photovoltaic installation has become justified [1, 2].

The output characteristics of a photovoltaic panel depend essentially on the solar radiation to which it is subjected and its temperature, which makes the knowledge of these two parameters is very important. These two quantities can be

measured using sensors, also they can be estimated in order to minimize the number of sensors used which is a very important factor in the design of photovoltaic systems.

The model of a photovoltaic cell with a single diode is the most used thanks to the simplification of the equivalent electrical circuit which makes it possible to describe the behavior of the cell with the minimum of equations. For constant climatic conditions, this model has five parameters. In the case of variable climatic conditions, these parameters change in consequence. The estimation of the series and shunt resistance of the photovoltaic generator equivalent diagram is certainly beneficial to correctly evaluate its energy balance [3, 4].

In this work, in order to treat the characteristics and to analyze the impact of the variations of the quantities intervening from it from a practical point of view, we study the case of the photovoltaic panel TITAN-12-50 of ERCO-INSAT laboratory.

In the first part, we will be interested in the mathematical model of a photovoltaic cell, the developed model takes

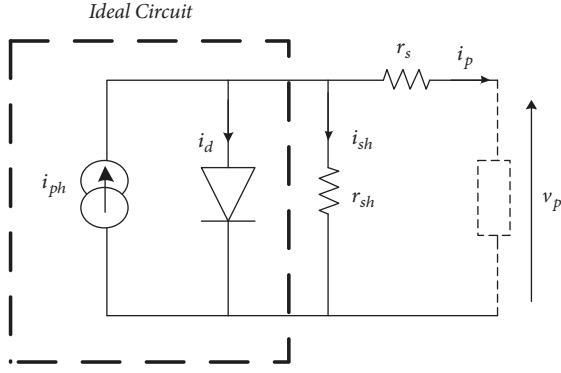


FIGURE 1: Equivalent circuit of real solar cell.

into account climatic variations such as temperature, solar radiation and wind speed. Support simulations are presented to show the dynamic behavior of the system. These simulations show that the shunt and series resistances are influenced by the climatic parameters or the interest of estimating them in real time. In the second part the expression of the two resistances has been developed. The efficiency of the new model has been validated experimentally while using a Dspace1104 card. The third part revolves around the estimation of two main parameters (solar radiation and temperature) through an algebraic strategy from an experimental curve $I_{pv}(V_{pv})$. Finally, we did a case study on the TITAN 12-50 panel installed on the roof of the ERCO-INSAT research unit.

2. Modeling of Solar Cell and Experimental Database

The equivalent circuit of a photovoltaic cell is given by Figure 1.

In the sense of this model, we can write the following relation:

$$i_{ph} = i_d + i_{pv} + i_{sh} = i_d + i_{pv} + \frac{v_{pv} + r_s i_{pv}}{r_{sh}} \quad (1)$$

with v_{pv} and i_{pv} being, respectively, the output voltage and the output current of PV cell. r_s and r_{sh} are the series and shunt resistors of the cell, i_{sh} is the current passing in the r_{sh} resistance, and i_d is the current of the diode.

The current of the diode i_d is strongly related to the temperature and the gap energy of the junction. It also depends on the voltage across the diode. It is given by the equation below:

$$i_d = i_s \left(\exp \left(\frac{v_{pv} + r_s i_{pv}}{v_t} \right) - 1 \right) \quad (2)$$

where i_s is the reverse saturation current of the diode and v_t is the solar cell thermal voltage.

The inverse saturation current and the thermal voltage are given by the following equations:

$$i_s = i_s(T_j) = i_{sr} \left(\frac{T_j}{T_{jr}} \right)^3 \exp \left(w_g \left(\frac{1}{v_{tr}} - \frac{1}{v_t} \right) \right) \quad (3)$$

$$v_t = \frac{\mathcal{K}_I \mathcal{K}_B T_j}{q}, \quad (4)$$

$$v_{tr} = \frac{\mathcal{K}_I \mathcal{K}_B T_{jr}}{q}$$

where $v_{tr} = \mathcal{K}_I \mathcal{K}_B / q$.

We note here that the index (r) used in this paper indicates that the value corresponds to the STC condition (Standard Test Condition: $E = E_s = 1000 \text{ W/m}^2$, $T_A = T_{Ar} = 25^\circ \text{C}$).

w_g is the energy of gap, \mathcal{K}_B Boltzmann constant, \mathcal{K}_I coefficient of ideality, and q the electron charge, and the main variable of this model is the temperature of the p-n junction of the diode T_j (expressed in $^\circ \text{K}$).

The following model was adopted taking into account variations in solar radiation, wind speed, and ambient temperature T_A .

$$T_j = T_A (^\circ \text{C}) + 273.15 + 33.75 E_s f_W(\vartheta_W) \quad (5)$$

The solar radiation E_s is expressed in W/m^2 and the function $f_W(\vartheta_W)$ introduces the effect of the wind speed.

$$f_W(\vartheta_W) = \exp(-\gamma(\vartheta_W - 1)) \quad \vartheta_W \geq 1 \quad (6)$$

The parameter γ must be positive for the function to vary in the opposite direction of the wind speed. Indeed the increase of the wind speed makes the solar cell cool [5].

The current of solar photons i_{ph} is strongly dominated by a variation of solar radiation and very slightly variable under the effect of the temperature. Given these properties, the current of photons is governed by the following model.

$$i_{ph} = i_{ph}(E_s, T_j) = E_s [i_{phr} + k_T (T_j - T_{jr})] \quad (7)$$

k_T is the temperature coefficient that depends a lot on the manufacturing technology and it is basically provided by the manufacturer.

Table 1 gives the values of the different quantities used in PVG model.

All the quantities related to the climatic conditions are defined. The electrical behavior in charge of the solar cell will be described by (8).

$$f(v_{pv}, i_{pv}) = i_{pv} - i_{ph} + i_s \left(\exp \left(\frac{v_{pv} + r_s i_{pv}}{v_t} \right) - 1 \right) + \frac{v_{pv} + r_s i_{pv}}{r_{sh}} \quad (8)$$

This function is a nonlinear function and involves several variables. In order to resolve it, we need a numerical method; in this work Newton-Raphson method is exploited [6].

The nominal powers of solar cells are always limited to a few watts. So the solution in this case is to switch to serial-parallel coupling of several cells. Solar energy is marketed in the form of panels or photovoltaic generator [7–9].

A PVG is a configuration comprising Np rows in parallel; each of the rows is formed by Ns panels in series, with each

TABLE 1: Quantities related to the physical model of the solar cell.

Notation	Designation	Numerical values
E_{sr}	Reference solar radiation (w/m ²) in STC	1000
T_{Ar}	Ambient temperature (°C) in STC	25
T_{jr}	Reference junction temperature (°K) in STC	298.15
w_g	Energy of gap (eV)	1.12
q	Electron charge (C)	1.602×10^{-19}
K_B	Boltzmann constant (J/°K)	1.38065×10^{-23}
K_I	Constant of ideality	1==>2
k_T	Temperature coefficient (A/°C)	0.0032

panel being itself formed of ns series cells. So we finally get the following.

$$\begin{aligned} I_{pv} &= i_{pv} \times N_p, \\ V_{pv} &= n_s \times N_s \times v_{pv} \end{aligned} \quad (9)$$

For this purpose, we denote, respectively, by I_{pv} and V_{pv} the current and the voltage of PVG.

So, finally we get for a photovoltaic generator the following mathematical model (10):

$$\begin{aligned} F(I_p, V_p) &= I_p - I_{ph} + I_s \left(\exp\left(\frac{V_p + R_s I_p}{V_t}\right) - 1 \right) \\ &+ \frac{V_p + R_s I_p}{R_{sh}} = 0 \end{aligned} \quad (10)$$

with

$$\begin{aligned} R_s &= \frac{N_s n_s r_s}{N_p} \\ R_{sh} &= N_s n_s r_{sh} \\ I_s &= N_p i_s \\ I_{ph} &= N_p i_{ph} \\ V_T &= N_s n_s v_T. \end{aligned} \quad (11)$$

2.1. Nonlinear Characteristic $I_{pv} = f(V_{pv})$. The mathematical model of a photovoltaic generator is expressed in the following form.

$$f = I_{pv} - I_{ph} - I_s + \mathcal{F}_s + \mathcal{F}_{sh} = 0 \quad (12)$$

To arrange the calculation in the simplest way and therefore as clear as possible, we will define the following quantities.

$$\mathcal{F}_s(V_{pv}, I_{pv}) = I_s \exp\left(\frac{V_{pv} + R_s I_{pv}}{V_T}\right) \quad (13)$$

$$\mathcal{F}_{sh}(V_{pv}, I_{pv}) = \frac{V_{pv} + R_s I_{pv}}{R_{sh}} = G_{sh}(V_{pv} + R_s I_{pv}) \quad (14)$$

We must solve the following system with two variables V_{pv} and I_{pv} .

$$f(V_{pv}, I_{pv}) = I_{pv} - I_{ph} - I_s + \mathcal{F}_s + \mathcal{F}_{sh} = 0 \quad (15)$$

This function is nonlinear; the most appropriate method for its resolution is the method of "Newton Raphson". This technique requires the development of the Jacobian matrix. The elements of this matrix are defined below.

$$J = \begin{bmatrix} \frac{\partial f}{\partial I_{pv}} & \frac{\partial f}{\partial V_{pv}} \end{bmatrix} \quad (16)$$

$$\frac{\partial f}{\partial I_{pv}} = 1 + \frac{R_s \mathcal{F}_s}{V_t} + R_s G_{sh} \quad (17)$$

$$\frac{\partial f}{\partial V_{pv}} = \frac{\mathcal{F}_s}{V_t} + G_{sh}$$

Table 2 gives the main data of the solar panel TITAN-12-50.

2.2. Influence of Solar Radiation on the Classic Model. To show the influence of solar radiation on the $I_{pv} = f(V_{pv})$ characteristic from the previously developed database, the characteristics are measured at the same constant temperature of 26°C and different solar radiation ranging from 200 to 900 W/m² as shown in Figure 2. It can be seen that the short-circuit current varies in the same direction as the solar radiation while the open circuit voltage varies slightly with the solar radiation.

2.3. Influence of Temperature on the Classic Model. For different temperatures and with a constant solar radiation equal to 600W/m², we acquire the voltage at the terminals of the PVG and the current flow as shown in Figure 3.

We notice that the short-circuit current is not sensitive to the variation of the temperature. On the other hand, the open circuit voltage varies in the opposite direction of the temperature.

3. Estimation of Series and Shunt Resistances

The estimation of the series and shunt resistances of the equivalent PVG scheme is certainly beneficial to correctly evaluate its energy balance.

3.1. Influence of Series Resistance on the Classic Model. For different values of the series resistance, the behavior of the PVG generator was simulated by plotting the $I_{pv} = f(V_{pv})$ characteristics. Figure 4 shows the evolution of the PV

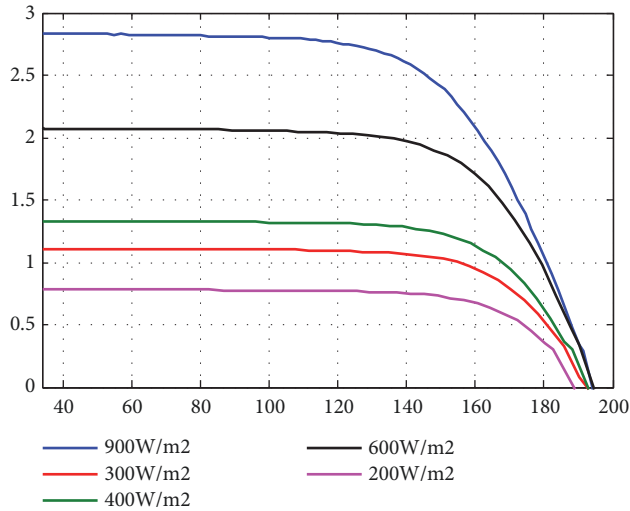


FIGURE 2: Influence of solar radiation on the $I_{pv} = f(V_{pv})$ characteristic.

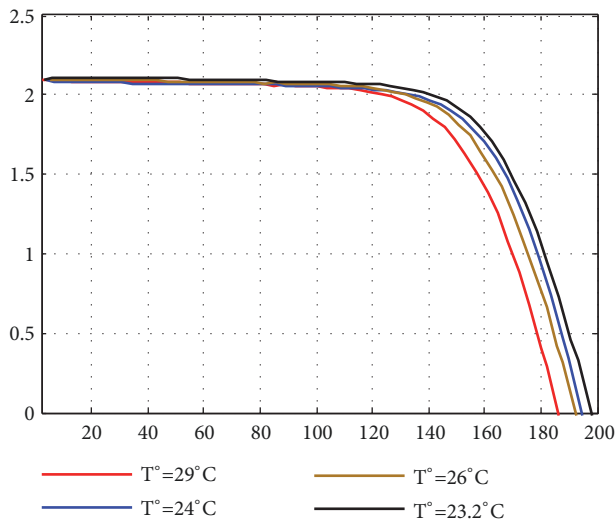


FIGURE 3: Influence of temperature on the $I_{pv} = f(V_{pv})$ characteristic.

current with the PV voltage for different values of series resistance.

It is noted that the short-circuit current and the open circuit voltage are not affected by the variation of the series resistance. On the other hand, the slope of the characteristic is very sensitive to this variation. The slope variation affects the maximum power as shown in Figure 5.

So, we can say here that the increase of the series resistance weakens the optimal power. This result is very obvious because a part of the power produced would be lost by Joule effect.

3.2. Influence of Shunt Resistance on the Classic Model. We will now set the value of the series resistance to see the influence of the shunt resistor, Figure 6.

TABLE 2: Electrical parameters of the solar panel TITAN-12-50.

Name	Manufacturer	TITAN
Description		STP-50-01
Cell types		Polycrystalline
Cell size		100cm ²
Cell number		36
Rated power		50Wc
Power tolerance		±5%
Optimal voltage		17.2V
Optimal current		2.9A
Open circuit voltage		21V
Short circuit current		3.4A
Efficiency		11.3%
Manufacturer's warranty		20 years

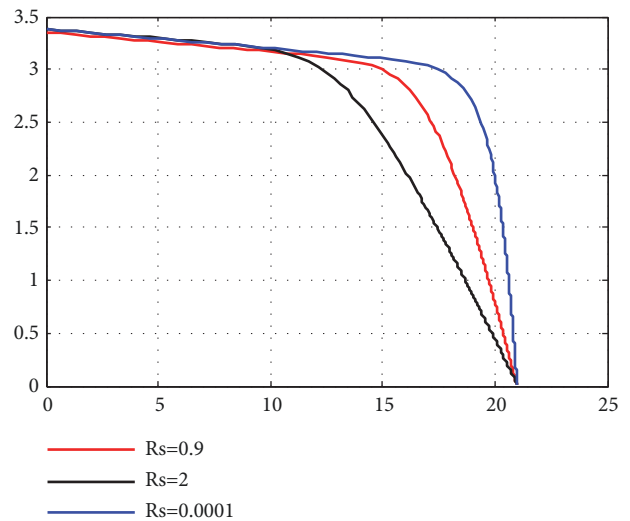


FIGURE 4: Influence of series resistance on the $I_{pv} = f(V_{pv})$ characteristic.

Like the series resistor, the shunt resistor also does not have an influence on the open circuit voltage and the short-circuit current. The effect of the shunt resistor is very focused on the optimum operating point of the PVG, Figure 7.

The increase in shunt resistance slightly weakens the optimal power. The joules losses due to the shunt resistor remain much lower than those due to the series resistance.

I_{phr} and I_{sr} are, respectively, the saturation and photons currents in the reference regime. The values of these quantities are usually evaluated from two particular regimes. For the open circuit and short-circuit regimes, the experience confirms that the effect of series and shunt resistances is almost negligible regardless of the weather conditions.

In open circuit regime, we have the following.

$$\begin{aligned} V_{pv} &= V_{oc} \\ I_{pv} &= 0 \end{aligned} \quad (18)$$

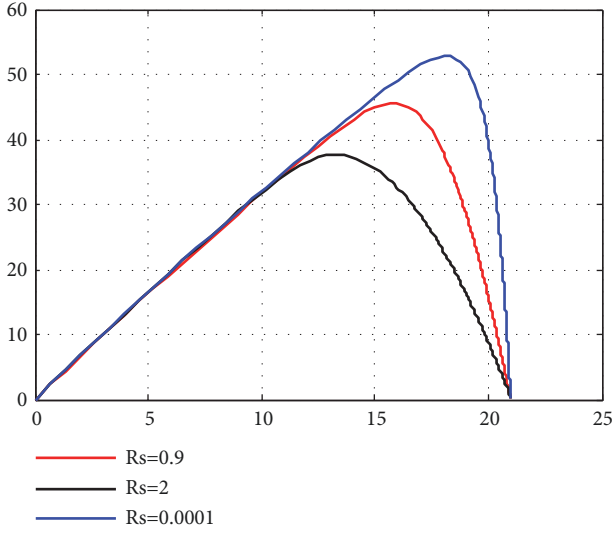


FIGURE 5: Influence of serie resistance on the $P_{pv} = f(V_{pv})$ characteristic.

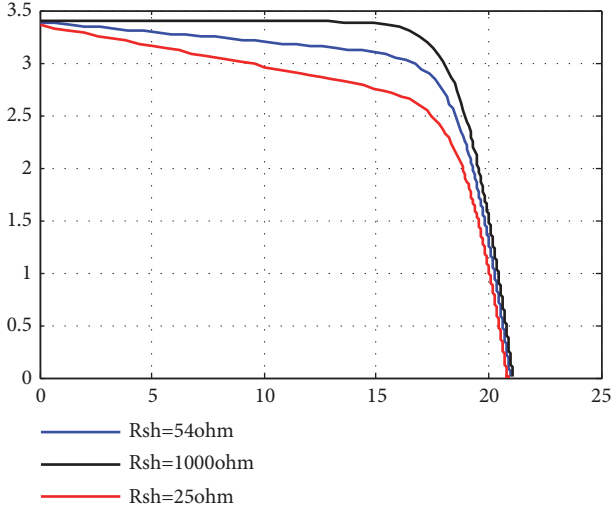


FIGURE 6: Influence of shunt resistance on the $I_{pv} = f(V_{pv})$ characteristic.

So, we obtain the following.

$$\begin{aligned}
 I_{ph} - I_d - I_{pv} - I_{sh} &= 0 \\
 I_{ph} - I_s \left(\exp\left(\frac{V_{oc}}{V_t}\right) - 1 \right) &= 0 \\
 I_{ph} &= I_s \left(\exp\left(\frac{V_{oc}}{V_t}\right) - 1 \right)
 \end{aligned} \tag{19}$$

In short-circuit regime, we have the following.

$$\begin{aligned}
 V_{pv} &= 0 \\
 I_{pv} &= I_{cc}
 \end{aligned} \tag{20}$$

So, we obtain the following.

$$I_{ph} = I_{cc} \tag{21}$$

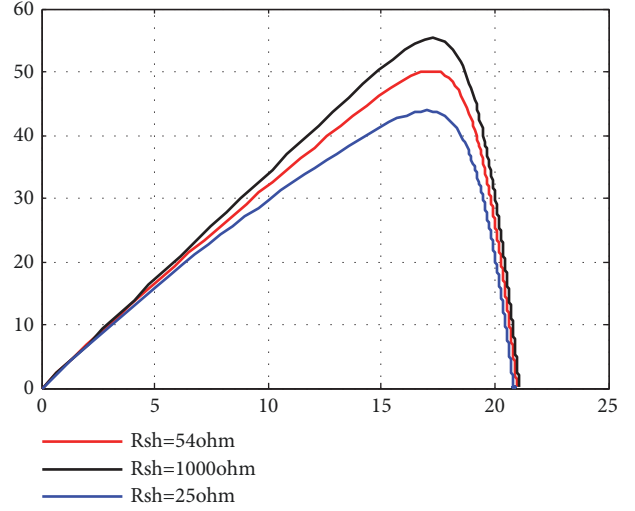


FIGURE 7: Influence of shunt resistance on the $P_{pv} = f(V_{pv})$ characteristic.

Back to the open circuit regime, we can write the following in reference climatic condition.

$$I_{sr} = \frac{I_{phr}}{\left(\exp(V_{ocr}/V_{tr}) - 1\right)} = I_{ccr} \exp\left(-\frac{V_{ocr}}{V_{tr}}\right) \tag{22}$$

3.3. Estimation of Series Resistance. The internal conductance of the photovoltaic generator in any mode satisfies the relation below.

$$G_{pv}(V_{pv}, I_{pv}) = \frac{\partial I_{pv}}{\partial V_{pv}} = -\frac{G_{sh}V_T + \mathcal{F}_s}{V_T + R_s \mathcal{F}_s + V_T R_s G_{sh}} \tag{23}$$

To estimate the value of the series resistor, it is necessary to carry out an open circuit test because the effect of the series resistance is manifested in the vicinity of the open circuit operation, unlike the effect of the shunt resistor, which remains insignificant. The value of the series resistance is estimated by the following relation.

$$R_s = -\frac{\partial V_{pv}}{\partial I_{pv}} \quad \text{when } I_{pv} = 0 \text{ and } V_{pv} = V_{oc} \tag{24}$$

By applying (23) in (24), we can deduce the following.

$$\begin{aligned}
 R_s &= -\frac{1}{G_{pv}(V_{oc}, 0)} = \frac{V_t}{I_s \exp(V_{oc}/V_t)} \\
 &= \frac{V_t}{I_s} \exp\left(-\frac{V_{oc}}{V_t}\right)
 \end{aligned} \tag{25}$$

Under Standard Test Conditions (STC), we consider the following peer relationship.

$$R_{sr} = \frac{V_{tr}}{I_{sr}} \exp\left(-\frac{V_{ocr}}{V_{tr}}\right) \tag{26}$$

Applying the expression of I_{sr} , we obtain the following.

$$R_{sr} = \frac{V_{tr}}{I_{ccr}} \left(1 - \exp\left(-\frac{V_{ocr}}{V_{tr}}\right)\right) \tag{27}$$

3.4. Estimation of Shunt Resistance. The effect of the shunt resistor is significant around the point of short-circuit operation, so it is necessary to perform a short-circuit test to estimate this resistance.

The conductance G_{sh} has the following expression:

$$G_{sh} = -\frac{\partial I_{pv}}{\partial V_{pv}} \quad \text{when } I_{pv} = I_{cc} \text{ and } V_{pv} = 0 \quad (28)$$

or, in other terms,

$$G_{sh} = -\mathcal{G}_{pv}(0, I_{cc}) = \frac{G_{sh}V_t + \mathcal{F}_{scc}}{V_t + R_s\mathcal{F}_{scc} + V_tR_sG_{sh}} \quad (29)$$

$$\mathcal{F}_{scc} = \mathcal{F}_s(0, I_{cc}) = I_s \exp\left(\frac{R_s I_{cc}}{V_t}\right)$$

so, finally we get (30).

$$\begin{aligned} V_t R_s G_{sh}^2 + \left(R_s I_s \exp\left(\frac{R_s I_{cc}}{V_t}\right)\right) G_{sh} \\ - I_s \exp\left(\frac{R_s I_{cc}}{V_t}\right) = 0 \end{aligned} \quad (30)$$

It is a second-order equation, and its solution passes by the computation of the discriminate, in which the square of the saturation current is involved, which is a very small quantity. We can thus eliminate the second term of this equation and estimate the shunt resistance by the following.

$$R_{sh} = \sqrt{\frac{R_s V_t}{I_s} \exp\left(-\frac{R_s I_{cc}}{V_t}\right)} \quad (31)$$

In STC, this relation becomes as follows.

$$R_{shr} = \sqrt{\frac{R_{sr} V_{tr}}{I_{sr}} \exp\left(-\frac{R_{sr} I_{ccr}}{V_{tr}}\right)} \quad (32)$$

This relation shows on one side a term proportional to the temperature and on the other side a second term, which decreases exponentially with the temperature.

3.5. Validation of the Proposed Model: Checking of the Evolution of Open Circuit Voltage with Temperature. The manufacturer supplies, under STC conditions, a coefficient of sensitivity of the open circuit voltage versus the value temperature. So, we can write the following.

$$\begin{aligned} V_{oc} &= V_{ocr} - 0.0798(T_A - T_{Ar}) \\ &= 22.9950 - 0.0798T_A \end{aligned} \quad (33)$$

Moreover, in the sense of the model, the open circuit voltage verifies.

$$V_{oc} = V_T \log\left(1 + \frac{I_{ph}}{I_s}\right) \quad (34)$$

The curves in Figure 8 correspond, respectively, to formula (33) given by constructor and to formula (34). The difference between the two curves is acceptable.

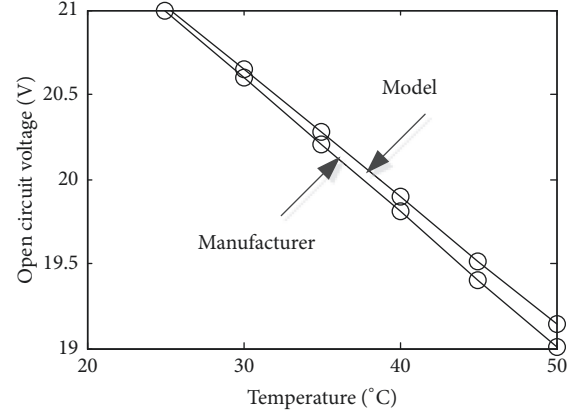


FIGURE 8: Variation of the open circuit voltage of the TITAN-12-50 panel with temperature.

3.6. Experimental Validation. To validate the previously proposed model, the photovoltaic panels installed at the research unit were exploited. The experimental installation comprises a photovoltaic generator whose characteristics are given in Table 2, a voltage sensor, a solar radiation sensor, and a temperature sensor. This experimental bench is controlled by a DS1104 dSPACE card.

The proposed strategy is implemented and tested in real time with a sampling frequency of 10 kHz. Figure 9 shows the complete configuration of the system described above.

Figures 10 and 11 show, respectively, the scenario of solar radiation and the comparison between the measured voltage and the voltage estimated by the developed model. It is constant that the tensions converge towards the same value whatever the variation of the solar radiation.

4. Estimation of Solar Radiation and Temperature

To measure the temperature, it is necessary to provide the solar panel with an integrated temperature sensor, which would greatly increase the cost on the one hand and complicate its manufacture on the other hand. A possible indirect solution for the junction temperature evaluation would be to identify it from the measurement results and establish a link with the ambient temperature.

With regard to solar radiation, the hardware solution of placing multiple solar radiation sensors would obviously increase the cost of installation [10–13]. The purpose of this section is to show the possibility of identifying the values of solar radiation and temperature from an experimental point of view.

Before going on to the method of the estimation of the solar radiation and the temperature for a photovoltaic system, we will present the notions of the adapted gradient method.

4.1. Quadratic Minimization by the Conjugate Gradient Method. The optimization, especially numerical optimization, has experienced a significant increase in recent years with the advent of the computer. It is often the last stage

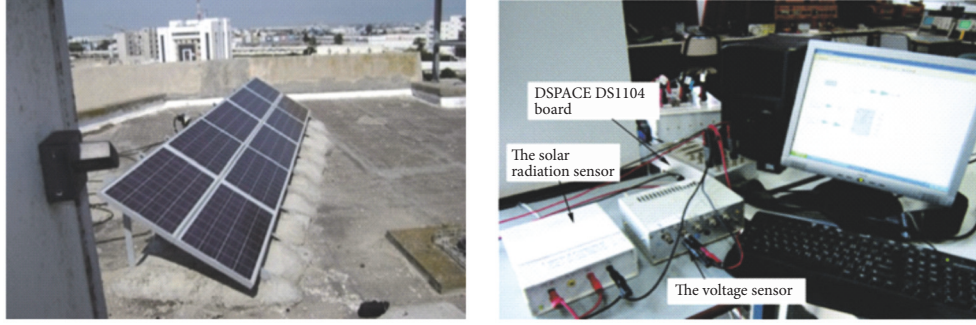


FIGURE 9: Configuration of the studied system.

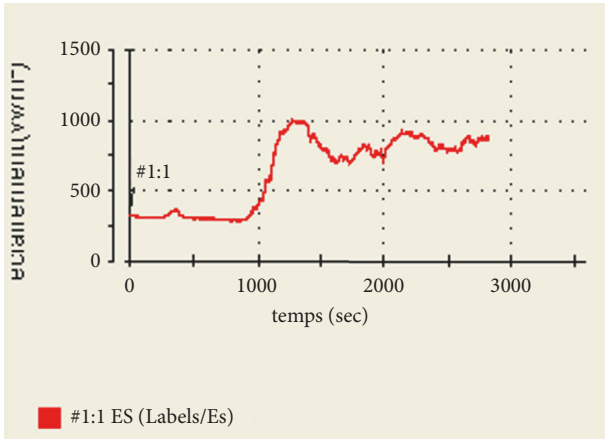
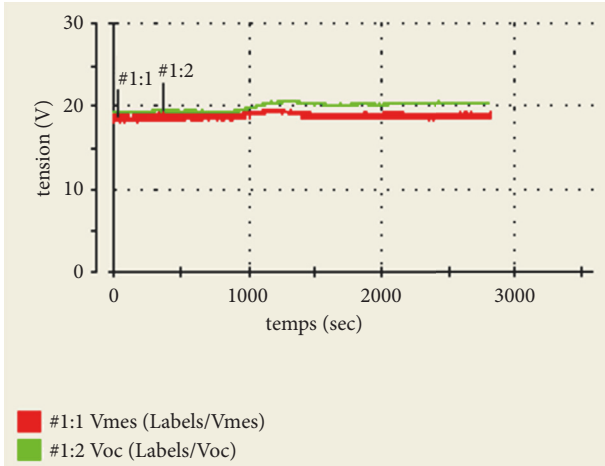


FIGURE 10: Variation of solar radiation.

FIGURE 11: Comparison between measured and estimated open circuit voltage (V_{oc} and V_{mes}).

of numerical analysis, where we have studied a physical phenomenon, put it into an equation, studied these equations, and shown that one could calculate the solutions with a computer. We begin to optimize the system by changing some parameters to change the solution in a desired direction.

Several methods are used for numerical optimization such as Newton's method, the quasi-Newton method, the conjugate gradient method, linear search, the regions of trust, and Nelder-Mead's method.

In this part, we will use the conjugate gradient method to minimize a nonlinear function $\Phi(\underline{X})$ differentiable at least twice.

The development of the Taylor series function $\Phi(\underline{X})$ around an initial condition \underline{X}_0 is expressed as follows.

$$\begin{aligned} \Phi(\underline{X}_0 + \underline{\Delta X}) \cong & \Phi(\underline{X}_0) + \sum_i \left. \frac{\partial \Phi}{\partial x_i} \right|_{\underline{X}_0} \Delta x_i \\ & + \frac{1}{2} \sum_{i,j} \left. \frac{\partial^2 \Phi}{\partial x_i \partial x_j} \right|_{\underline{X}_0} \Delta x_i \Delta x_j \end{aligned} \quad (35)$$

This equation can be further rewritten in the following form involving the gradient vector \underline{G} and the Hessian matrix H of the second derivatives evaluated in \underline{X}_0 . The Hessian matrix constitutes the Jacobian matrix of the gradient vector.

$$\Phi(\underline{X}_0 + \underline{\Delta X}) \cong \Phi(\underline{X}_0) + \underline{G}_0^T \underline{\Delta X} + \frac{1}{2} \underline{\Delta X}^T H_0 \underline{\Delta X} \quad (36)$$

$$\underline{G}_0 = \underline{G}(\underline{X}_0) = \left. \frac{\partial \Phi}{\partial \underline{X}} \right|_{\underline{X}_0} \quad (37)$$

$$H_0 = H(\underline{X}_0) = \left[\left. \frac{\partial \underline{G}(\underline{X})}{\partial \underline{X}} \right]_{\underline{X}_0}$$

In expanded form, the matrix $H(\underline{X})$ is symmetric and has the following expression.

$$h_{ij} = h_{ji} = \frac{\partial g_i}{\partial x_j} = \frac{\partial g_j}{\partial x_i} = \frac{\partial^2}{\partial x_i \partial x_j} = \frac{\partial^2}{\partial x_j \partial x_i} \quad (38)$$

The solution of minimizing a quadratic problem of the type below using the conjugate gradient method is given by the following system.

$$\begin{aligned} & \min_{\underline{X}} \Phi(\underline{X}) \\ \Phi(\underline{X}) = & \frac{1}{2} \underline{X}^T H \underline{X} + \underline{C}^T \underline{X} \end{aligned} \quad (39)$$

To minimize the function $\Phi(\underline{X})$ we could proceed to a local minimization in terms of $\Delta \underline{X}$ with \underline{G}_0 and H_0 constant and repeat the same calculation as many times as necessary by rectifying each time the initial condition, the gradient vector, and the Hessian matrix. Obviously, it is admitted here that the Hessian matrix remains positive, which is often the case.

4.2. Estimation of Solar Radiation and Temperature: Minimizing the $V_p(I_p)$ Function. In this section, we are interested in the identification of E_s and V_t parameters from a given (V_{pv}, I_{pv}) operating point.

As we have already presented in the first section, the model of a photovoltaic generator is described by the following.

$$f = I_p - I_{ph} - I_s + \mathcal{F}_s + \mathcal{F}_{sh} = 0 \quad (40)$$

The different terms of this model are defined as follows.

$$\begin{aligned} V_T &= \eta T_j \\ V_{Tr} &= \eta T_{jr} \\ I_{ph} &= E_s [I_{ccr} + K_{Tr} (V_T - V_{Tr})] \\ I_s &= I_{sr} \left(\frac{V_T}{V_{Tr}} \right)^3 \exp \left(\frac{W_g}{V_{Tr}} - \frac{W_g}{V_T} \right) \\ \mathcal{U}_p &= V_p + R_s I_p \\ \mathcal{F}_s &= I_s \exp \left(\frac{\mathcal{U}_p}{V_T} \right) \\ \mathcal{F}_{sh} &= G_{sh} \mathcal{U}_p \end{aligned} \quad (41)$$

The main variables of this model are, respectively, the voltage across the generator V_p and the current I_p delivered to the load. These quantities vary, of course, with the load, solar irradiance, and temperature. The solar radiation is denoted here as E_s . The junction temperature appears by the magnitude V_T , which is proportional to it, provided that the factor of constant ideality is considered. The parameters R_s and G_{sh} correspond, respectively, to the series resistance and the shunt conductance of the equivalent scheme. The other parameters are constants.

The mathematical model of a photovoltaic generator for a given operating point becomes as follows.

$$f(V_T, E_s) = 0 \quad (42)$$

Before exposing the identification technique used, it is necessary to develop the first and second derivatives of the terms of the function f of the model with respect to these parameters. We establish the following.

$$\begin{aligned} u_p &= V_{pv} + R_s I_{pv} \\ \frac{\partial I_{ph}}{\partial V_t} &= E_s K_{Tr} \\ \frac{\partial I_{ph}}{\partial E_s} &= I_{ccr} + K_{Tr} (V_t - V_{tr}) \end{aligned}$$

$$\frac{\partial I_s}{\partial V_t} = I_s \left(\frac{3V_t + W_g}{V_t^2} \right)$$

$$\frac{\partial \mathcal{F}_s}{\partial V_t} = \mathcal{F}_s \left(\frac{3V_t + W_g - u_p}{V_t^2} \right)$$

$$\frac{\partial^2 I_{ph}}{\partial E_s^2} = \frac{\partial^2 I_{ph}}{\partial V_t^2} = 0$$

$$\frac{\partial^2 I_s}{\partial V_t^2} = I_s \left(\frac{(2V_t + W_g)^2 + 2V_t^2}{V_t^4} \right)$$

$$\frac{\partial^2 \mathcal{F}_s}{\partial V_t^2} = \mathcal{F}_s \left(\frac{(2V_t + W_g - u_p)^2 + 2V_t^2}{V_t^4} \right)$$

(43)

Let us consider an experimental point (V_{pv}, I_{pv}) raised to solar radiation and temperature supposed unknown. The injection of this point into the function f of the mathematical model (40) would lead to a nonzero value because of the error between the real values of the parameters and the values used in the model.

By denoting by \underline{X} the vector of the parameters (V_t, E_s) to be identified, the function (40) of the model would be denoted accordingly by $f(\underline{X})$. The object is to determine the vector \underline{X} that makes $f(\underline{X})$ tend to zero.

In order to take advantage of the available digital quadratic programming tools, we perform the minimization of the following quadratic criterion.

$$\Phi(\underline{X}) = \frac{1}{2} f^2(\underline{X}) \quad (44)$$

The Taylor series development expresses $\Phi(\underline{X})$ as follows:

$$\Phi(\underline{X}_0 + \underline{x}) = \Phi(\underline{X}_0) + \underline{G}_0 \underline{x} + \frac{1}{2} \underline{x} H_0 \underline{x} \quad (45)$$

where \underline{G}_0 and H_0 are, respectively, the gradient vector and the Hessian matrix of $\Phi(\underline{X})$ around an initial condition \underline{X}_0 . The vector \underline{x} corresponds to the variation to be made around \underline{X}_0 .

The gradient vector and the Hessian matrix are expressed as follows.

$$\underline{G}(\underline{X}) = \frac{\partial \Phi}{\partial \underline{X}} = f(\underline{X}) \frac{\partial f(\underline{X})}{\partial \underline{X}} \quad (46)$$

$$H(\underline{X}) = \frac{\partial \underline{G}(\underline{X})}{\partial \underline{X}}$$

By involving the sensitivity relationships defined above, the gradient vector $\underline{G}(\underline{X})$ has for relation (47) the following.

$$\begin{aligned} \psi_1 &= \frac{\partial f}{\partial V_t} = \frac{\partial I_{pv}}{\partial V_t} - \frac{\partial I_{ph}}{\partial V_t} - \frac{\partial I_s}{\partial V_t} + \frac{\partial \mathcal{F}_s}{\partial V_t} + \frac{\partial \mathcal{F}_{sh}}{\partial V_t} \\ &= -\frac{\partial I_{ph}}{\partial V_t} - \frac{\partial I_s}{\partial V_t} + \frac{\partial \mathcal{F}_s}{\partial V_t} \end{aligned}$$

$$\begin{aligned}
&= -E_s K_{tr} - I_s \left(\frac{3V_t + W_g}{V_t^2} \right) \\
&\quad + \mathcal{F}_s \left(\frac{3V_t + W_g - u_p}{V_t^2} \right) \\
\psi_2 &= \frac{\partial f}{\partial E_s} = \frac{\partial I_{pv}}{\partial E_s} - \frac{\partial I_{ph}}{\partial E_s} - \frac{\partial I_s}{\partial E_s} + \frac{\partial \mathcal{F}_s}{\partial E_s} + \frac{\partial \mathcal{F}_{sh}}{\partial E_s} \\
&= -\frac{\partial I_{ph}}{\partial E_s} = -[I_{ccr} + K_{Tr}(V_t - V_{tr})] \\
\underline{G} &= \begin{bmatrix} \psi_1 \\ \psi_2 \end{bmatrix}
\end{aligned} \tag{47}$$

In order to simplify the calculation without losing too much on precision, the Hessian matrix could be expressed by the approximate Gaussian relation below.

$$H(\underline{X}) \simeq \left(\frac{\partial f(\underline{X})}{\partial \underline{X}} \right) \left(\frac{\partial f(\underline{X})}{\partial \underline{X}} \right)^T = \begin{bmatrix} \psi_1^2 & \psi_1 \psi_2 \\ \psi_1 \psi_2 & \psi_2^2 \end{bmatrix} \tag{48}$$

We can express exactly this matrix by the use of the following complete formula.

$$\begin{aligned}
H &= \begin{bmatrix} \psi_1 + \psi_3 f & \psi_1 \psi_2 - K_{Tr} f \\ \psi_1 \psi_2 - K_{Tr} f & \psi_2^2 \end{bmatrix} \\
\psi_3 &= \frac{\partial \psi_1}{\partial V_t} = \frac{\partial}{\partial V_t} \left(\frac{\partial f}{\partial V_t} \right) \\
&= \frac{\partial}{\partial V_t} \left(-\frac{\partial I_{ph}}{\partial V_t} - \frac{\partial I_s}{\partial V_t} + \frac{\partial \mathcal{F}_s}{\partial V_t} \right) = -\frac{\partial^2 I_s}{\partial V_t^2} + \frac{\partial^2 \mathcal{F}_s}{\partial V_t^2} \\
&= -I_s \left(\frac{(2V_t + W_g)^2 + 2V_t^2}{V_t^4} \right) \\
&\quad + \mathcal{F}_s \left(\frac{(2V_t + W_g - u_p)^2 + 2V_t^2}{V_t^4} \right)
\end{aligned} \tag{49}$$

The proposed technique is to iteratively apply the conjugate gradient method using $H(\underline{X})$ and $\underline{G}(\underline{X})$ as parameters of the quadratic problem. The algorithm consists of the following steps:

- (i) Give an initial condition \underline{X}_0 for the parameter vector \underline{X} .
- (ii) Calculate $\underline{G}(\underline{X}_0)$ and $H(\underline{X}_0)$ and readjust the limits of the variation vector \underline{x} .
- (iii) To seek the optimal solution of the quadratic problem by the constrained conjugate gradient technique to establish the correction \underline{x} necessary for the minimization of $\Phi(\underline{X})$ around \underline{X}_0 .

$$\min_{\underline{x}} \left(\frac{1}{2} \underline{x}^T H \underline{x} + \underline{G}^T \underline{x} \right) \tag{50}$$

$$\underline{x}_{min} \leq \underline{x} \leq \underline{x}_{max}$$

- (iv) Correct the parameter vector by $\underline{X}_0 = \underline{X}_0 + \underline{x}$ and return to step (ii).

TABLE 3: Different experimental values of the characteristics (V_{pv} , I_{pv}).

V_{pv}	I_{pv}
0	3.300
3.5353	3.2505
5.5500	3.2010
6.7962	3.1680
8.3215	3.1185
9.7205	3.0690
10.9567	3.0195
12.2502	2.9535
13.8727	2.8545
15.2266	2.7555
16.5322	2.5740
17.2528	2.4255
17.9818	2.1945
18.4340	1.9800
18.7883	1.7655
19.1226	1.5345
19.3951	1.3200
19.6467	1.1055
19.8972	0.8745
20.1202	0.6600
20.3465	0.4455
20.5306	0.2145
20.6500	0

4.3. Estimation of T_j and E_s (Application on the Photovoltaic Panel TITAN 12-50). Just to fix the ideas and check the relations, consider the constant parameters of the Table 1 and a function point corresponding to $V_p = 13.8727V$ and $I_p = 2.8545A$. Propose as initial conditions $\underline{X}_0 = [1.3 \ 1] = [V_T \ E_s]_0$.

With this initial condition, we calculate the following.

$$f_0 = -0.3045$$

$$\underline{G}_0 = \begin{bmatrix} -0.0580 \\ 0.9743 \end{bmatrix} \tag{51}$$

$$H_0 = \begin{bmatrix} 0.0362 & -0.6092 \\ -0.6092 & 10.2387 \end{bmatrix}$$

By completing the algorithm flow with the limits

$$\begin{bmatrix} 1 \\ 0.8 \end{bmatrix} \leq \underline{X} \leq \begin{bmatrix} 1.6 \\ 1.2 \end{bmatrix} \tag{52}$$

we reach the solution: $\underline{X} = [1.3056, 0.9052]$

$$V_T = 1.3056 \text{ and } E_s = 0.9052.$$

We note here that the estimated value of the solar radiation is divided by a ratio of 1000. Still as a test and validation of the developments made, consider the complete curve (V_{pv} , I_{pv}) given by Table 3 with the parameters of the TITAN-12-50 module already introduced in Table 2.

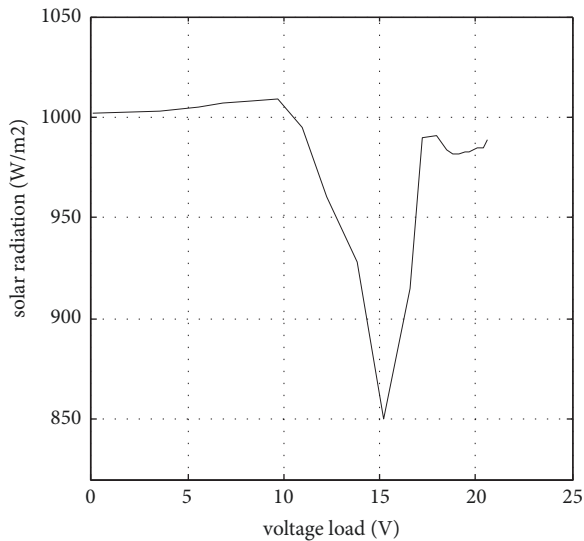


FIGURE 12: Variation of solar radiation with the load voltage.

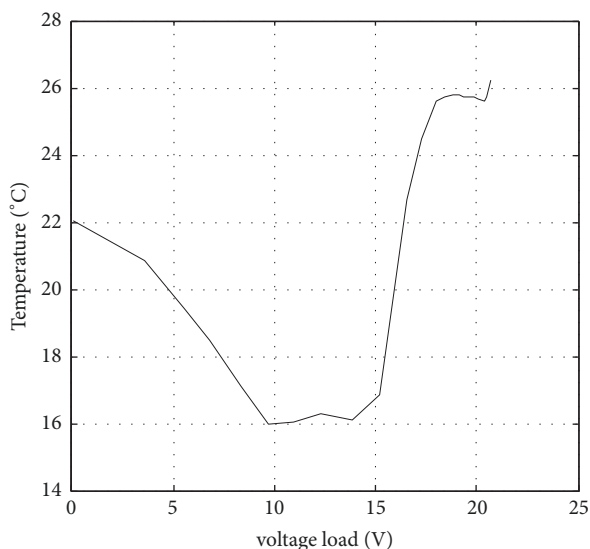


FIGURE 13: Variation of temperature with the load voltage.

Figures 12 and 13 give, respectively, the variation of solar radiation and the temperature with the load voltage

5. Conclusion

In this paper, we have proposed a method based on numerical development to estimate through an experimental curve the two main parameters influencing the operation of a PV system. In the same way, we estimated the two series and shunt resistors while showing the influence of the climatic conditions on these resistances, which allows us to develop a new model of a PVG. Finally, we showed the efficiency of this model experimentally using dSPACE 1104.

Data Availability

The parameters of the photovoltaic panel are included in the article, while the simulation programs used in the study are available from the corresponding author on request.

Conflicts of Interest

The authors declare that there are no conflicts of interest regarding the publication of this paper.

References

- [1] R. Gammoudi, N. Rebei, and O. Hasnaoui, "STM microcontroller implementation of MPPT algorithms for stand-alone PV Water Pumping System," *International Journal of Engineering and Technical Research (IJETR)*, 2015.
- [2] G. Lavidas and V. Venugopal, "Prospects and applicability of wave energy for South Africa," *International Journal of Solar Energy*, 2017.
- [3] R. A. M. Coetzee, A. Mwesigye, and Z. Huan, "A numerical model for optimal receiver array and mass flow rate in residential solar water heating systems," *International Journal of Sustainable Energy*, vol. 37, no. 9, pp. 902–918, 2017.
- [4] Y. V. Daus, I. V. Yudaev, and G. V. Stepanchuk, "Reducing the costs of paying for consumed electric energy by utilizing solar energy," *Applied Solar Energy*, vol. 54, no. 2, pp. 139–143, 2018.
- [5] N. Rebei, A. Hmidet, R. Gammoudi, and O. Hasnaoui, "Implementation of photovoltaic water pumping system with MPPT controls," *Frontiers in Energy*, vol. 9, no. 2, pp. 187–198, 2015.
- [6] H. Brahmi and R. Dhifaoui, "Dynamic characteristics and improved MPPT control of PV generator," *Frontiers in Energy*, vol. 7, no. 3, pp. 342–350, 2013.
- [7] R. H. Almeida, L. Narvarte, and E. Lorenzo, "PV arrays with delta structures for constant irradiance daily profiles," *Solar Energy*, vol. 171, pp. 23–30, 2018.
- [8] Y. V. Daus and V. V. Kharchenko, "Evaluating the applicability of data on total solar-radiation intensity derived from various sources of actinometric information," *Applied Solar Energy*, vol. 54, no. 1, pp. 71–76, 2018.
- [9] S. V. Kiseleva, O. S. Popel', A. B. Tarasenko, and R. R. Avezov, "Efficiency estimation for the grid-tie photovoltaic stations construction in some regions of Central Asia and Transcaucasia," *Applied Solar Energy*, vol. 53, no. 4, pp. 306–311, 2017.
- [10] F. dell'Isola, M. Cuomo, L. Greco, and A. Della Corte, "Bias extension test for pantographic sheets: numerical simulations based on second gradient shear energies," *Journal of Engineering Mathematics*, vol. 103, pp. 127–157, 2017.
- [11] J. Kaderli, J. Zweck, A. Safin, and S. E. Minkoff, "An analytic solution to the coupled pressure-temperature equations for modeling of photoacoustic trace gas sensors," *Journal of Engineering Mathematics*, vol. 103, pp. 173–193, 2017.
- [12] R. R. Avezov, E. Y. Rakhimov, and A. M. Mirzabaev, "Calculation of the temperature of the internal surface of the heat-removing channel wall of the ray-absorbing heat-exchange panels of flat-plate solar water-heating collectors," *Applied Solar Energy*, vol. 53, no. 4, pp. 312–315, 2017.
- [13] S. Franco, V. R. Mandla, and K. R. Mohan Rao, "Estimation of bright roof areas for large scale solar PV applications to meet the power demand of megacity Hyderabad," *Applied Solar Energy*, vol. 52, no. 4, pp. 284–289, 2016.




Hindawi

Submit your manuscripts at
www.hindawi.com

